*Journal of Molecular Cell Biology* (2022), 14(3), mjac012 https://doi.org/10.1093/jmcb/mjac012
Published online March 3, 2022

Application Note

# Synaptic degeneration in the prefrontal cortex of a rat AD model revealed by volume electron microscopy

Alzheimer's disease (AD), a neurodegenerative disease, is identified as the most common cause of dementia (Goedert and Spillantini, 2006). Typical symptoms of AD in neuropathology are closely associated with changes in synapses and neurons (Serrano-Pozo et al., 2011). The prefrontal cortex (PFC) plays a crucial role in executive function, controlling the highest level of cognitive and emotional processes, and is also vulnerable to neurodegeneration in AD (Salat et al., 2001). While synaptic degeneration is believed to underlie the progressive decline of cognition in AD, specific changes in synaptic structures relevant to AD remain elusive due to a shortage of quantitative tools. Synaptic dysfunction, while key to AD pathophysiology, is difficult to monitor and study in human AD patients. The existing technologies, such as cerebrospinal fluid or blood biomarkers, magnetic resonance imaging, and positron emission tomography, can only indirectly infer synaptic changes in the brain. Thus, it is critical to have an animal model that resembles closely human AD. The newly developed AD rat model, the amyloid precursor protein (*App*) knock-in rat line harboring Swedish–Beyreuther/Iberian–Arctic mutations (homozygous $App^{NL\text{-}G\text{-}F}$ rat), offers a great opportunity (Pang et al., 2021). Electron microscopy (EM) has been the method of choice to study the ultrastructure of synapses. While allowing magnification of images by a million times, this conventional EM provides snapshots, rather than quantitative measures, of ultrastructural details of synapses. With the development of automated tape-collecting ultramicrotome (ATUM; Baena et al., 2019) and artificial intelligence (AI)-assisted 3D reconstruction of scanning electron microscopy (SEM) images (Motta et al., 2019), it is now possible to quantitatively characterize morphological features of synapses and dendrites in detail.

In this study, we performed a detailed analysis of the 3D ultrastructure of synapses and dendrites in layer 4 of the PFC between AD and wild-type (WT) rats. Brain samples were collected from 6-month-old male $App^{NL\text{-}G\text{-}F}$ rats and their WT littermates (Pang et al., 2021). Using ATUM–SEM (Supplementary Figure S1) and AI-assisted 3D reconstruction of the 3D ultrastructure of synapses and dendrites, we characterized in detail ultrastructural features of synaptic density, size, and postsynaptic targets (dendritic spine and shaft). Our results revealed alterations in synaptic density, synaptic apposition surface (SAS), and postsynaptic density (PSD) volume (Figure 1A; Supplementary Figure S2; see Supplementary material for details).

A typical synapse consists of a presynaptic terminal with synaptic vesicles, a synaptic cleft, and a postsynaptic unit (dendritic spine, dendritic shaft, or cell body) with an electron-dense PSD (Supplementary Figure S3A). PSD is located beneath the surface of the postsynaptic membrane and appears dark in an EM image (Supplementary Figure S3B, yellow boxes). Given that PSD is a unique feature of synapses, it was used to identify the site of synapses. Identification and reconstruction of synapses in the aligned EM volume were performed via a series of largely automated workflows (Supplementary Figure S3C; see Supplementary material for details).

All the synapses in the 3D EM volume of WT and AD rats were identified and reconstructed with a 90.46% recall rate and a 97.67% precision rate. In addition, all the synapses were 3D visualized with a pseudo-color (Figure 1B and C, 3D-PSD). A total of 11488 synapses were identified in WT rats (total tissue volume: 26049 $\mu m^3$) and a total of 19478 synapses were identified in AD rats (total tissue volume: 44627 $\mu m^3$).

At present, few studies have examined the alteration of synapses in the AD brain at a 3D ultrastructural level. Before 3D analysis, we first analyzed synapses of 2D images obtained via EM from the PFC of three WT and three AD rats (Supplementary Table S1). From 2D images, the number of synapses decreased slightly in the AD PFC, compared with that in the WT (Supplementary Figure S3D). We further analyzed reconstructed synapses in the 3D EM volume obtained from the PFC (excluding cell body and myelin; the analyzed volume: 20919 $\mu m^3$ for WT and 40727 $\mu m^3$ for AD). The volume density of the synapses was 0.549 synapses/$\mu m^3$ for WT and 0.478 synapses/$\mu m^3$ for AD, respectively (Figure 1D; Supplementary Table S2). Both 2D and 3D analyses indicated that there was a decrease in synapses in AD rats, consistent with changes of presynaptic vesicle clouds (0.512 clouds/$\mu m^3$ for WT and 0.403 clouds/$\mu m^3$ for AD; Supplementary Figure S4).

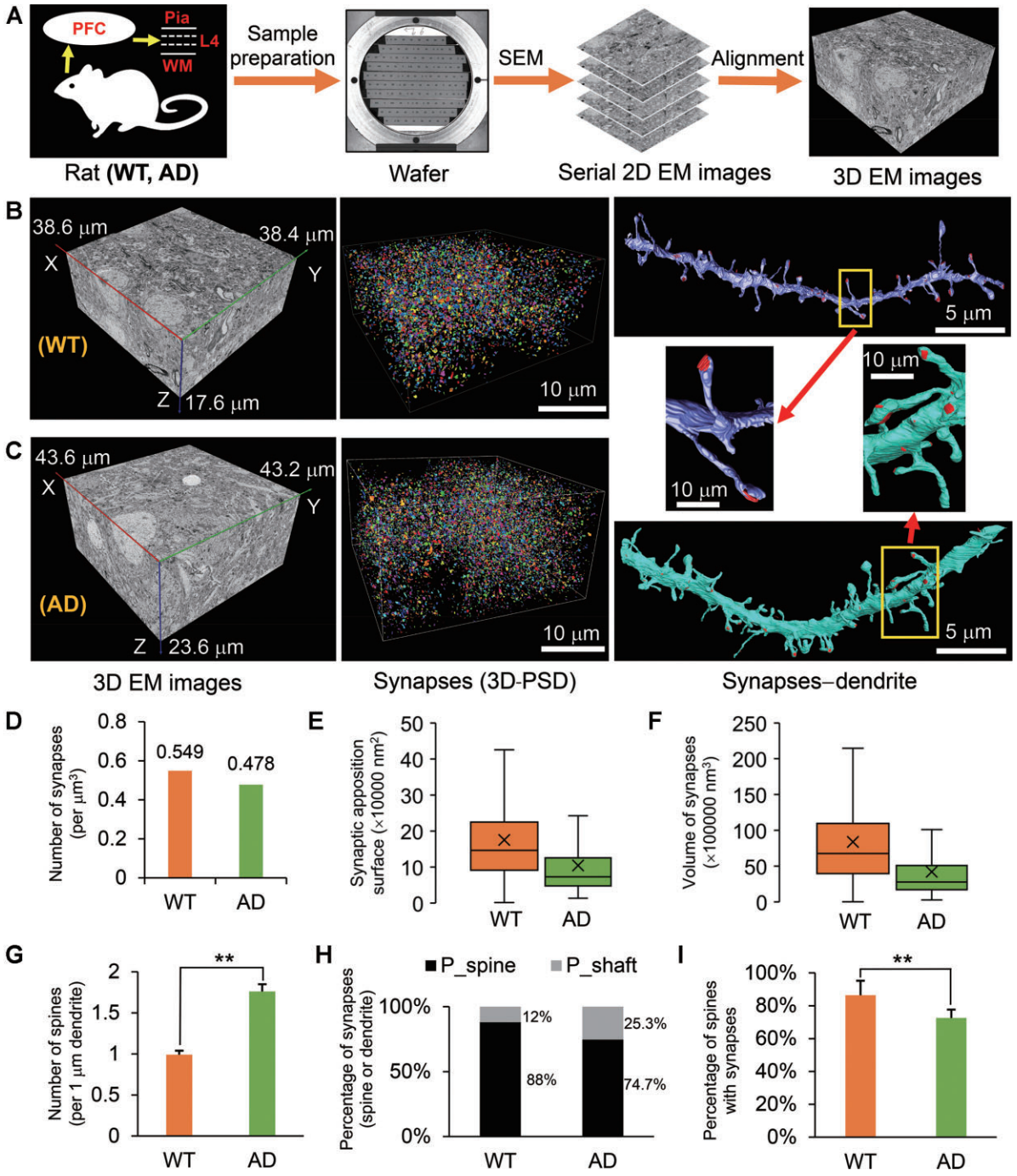


**Figure 1** 3D reconstruction and analysis of synapses and dendrites in layer 4 fields of PFC in the AD rat model. (**A**) Fresh PFC samples were excised from rat brains and rapidly fixed, washed, dehydrated, and embedded in resin. The samples were then sliced into ~50-nm sections using an ATUM and then collected on tapes. The tapes were then cut into strips and attached to a silicon wafer. The sections were imaged in an SEM instrument with 3 nm × 3 nm pixels. The serial 2D EM images were aligned to generate a 3D EM volume. (**B** and **C**) An aligned 3D EM volume and the corresponding reconstruction of synapses and dendrites of WT (top) and AD (bottom) rats, respectively. (**D**) The density of synapses within the 3D EM volume is greater in WT rats than in AD rats (per $\mu m^3$). (**E**) The mean of SAS is more prominent in WT rats than in AD rats. '×' indicates the mean. (**F**) The mean of synapse volume is greater in WT rats than in AD rats. '×' indicates the mean. (**G**) The number of dendritic spines per micrometer of dendrites. We counted 15 and 10 dendrites from WT and AD rats, respectively (Student's *t*-test, $^{**}P < 0.01$). (**H**) More synapses are formed on dendritic shafts in AD rats than in WT rats. Nonetheless, both are considerably fewer than synapses formed on dendritic spines. The statistical samples are the same as **G**. (**I**) A reduction in the percentage of spines with synapses in AD rats. The dendritic spines of AD rats are less likely to form synapses compared with that of WT rats (Student's *t*-test, $^{**}P < 0.01$). Data in bar graphs are presented as mean ± SD.

Synaptic degeneration is a critical pathophysiology in AD. Two critical components of the synaptic junction are the active zone (AZ) and PSD, which are related to presynaptic neurotransmitter release and postsynaptic responsiveness, respectively. The SAS describes the overlapping area between the AZ and PSD spatially. The AZ and PSD are in close apposition and positioned face to face, and their surface areas are highly similar (correlation coefficients exceeding 0.97; Schikorski and Stevens, 1997). Thus, the SAS can be viewed by a single surface of apposition between the AZ and PSD. In this study, we used one-sided surface area of PSD to represent the SAS and measured the SAS of all synapses in WT and AD rats. The SAS in the PFC of $App^{NL\text{-}G\text{-}F}$ rats was significantly reduced, compared with that in their WT littermates (Figure 1E; Supplementary Figure S3E and F), implying possible impairments in presynaptic neurotransmitter release and/or postsynaptic responsiveness. Moreover, structural changes in PSD may contribute to cognitive deficits in AD (Koffie et al., 2009). The volume of PSD in AD rats was significantly smaller than that in the WT (Figure 1F; Supplementary Figure S3G and H). We also found a linear relationship between SAS and the volume of synapses (reflected by PSD volume; Supplementary Figure S3I). Taken together, our 3D reconstruction analysis indicates that there is a slight but significant reduction in the number of synapses as well as a marked reduction in SAS and PSD volume in AD rats.

Neuronal dendrites include dendritic spines and dendritic shafts, the main postsynaptic components that harbor synaptic receptors. The size, shape, and density of dendritic spines are regulated by neuronal activity, and their changes are associated with the efficiency and plasticity of synapses (Leuner and Shors, 2013). Reconstructing the 3D structure of dendrites at nanoscale resolution can reveal the actual morphology of dendritic spines. In this study, we reconstructed dendrites through a series of largely automated techniques based on machine-learning methods (Supplementary Figure S5A; see Supplementary material for details). We extracted 15 and 10 dendrites from 3D reconstruction of neurons in WT and AD rats, respectively (Supplementary Figure S5B and E). Notably, the morphology of dendrites from WT rats was more in line with the reported morphology (Supplementary Figure S5C and D); moreover, most dendritic spines were mushroom-shaped. In contrast, dendrites of AD rats were irregular in shape, and dendritic spines were mostly thin (Supplementary Figure S5F and G). The reconstruction of dendrites showed that the AD PFC has more dendritic spines compared with the WT. This result suggests that AD caused an increase, rather than a decrease, in dendritic spines.

The paradoxical finding of the increase in the number of dendritic spines in AD rat brains prompted us to study in detail how synapses are distributed on dendrites. The site of synaptic formation on dendrites could be easily determined from 3D reconstruction of synapses and dendrites. Synapses were formed on either dendritic spines or dendritic shafts (Figure 1B and C; Supplementary Figure S6). There was a significant increase in the number of spines per micrometer in AD rats (Figure 1G). In both WT and AD rats, more synapses are present on dendritic spines than on dendritic shafts (Figure 1H). However, the proportion of spine synapses (those formed on spine heads) in AD rats was lower than that in the WT (Figure 1H; Supplementary Figure S6H). In other words, the increase in the number of synapses on dendritic shafts can imply an increase in inhibitory synapses in AD rats (Karimi et al., 2020). Thus, despite the increase in the total number of dendritic spines in AD rats, many thin spines did not form synapses (spines without synapses; Figure 1I), and thus were not involved in synaptic transmission. It is possible that pathological stimuli (such as Aβ or tau) trigger the formation of many thinner spines as a compensatory mechanism, leading to a perceived increase in spine number in the AD rat model. Thin and stubby spines have smaller PSD containing mainly N-methyl-D-aspartate receptors. By contrast, mushroom spines have larger PSD anchoring a higher density of α-amino-3-hydroxy-5-methyl-4-isoxazolepropionic acid receptors, stabilizing synaptic function.

Compared with low-resolution light microscopy, volume EM is better suited for accurate illustration and quantitative measurement of the dendritic spine and fine structure of synapses. In this study, we have investigated the synaptic structure of layer 4 of the PFC at a nanoscale level using a newly developed AD rat model. 3D volume EM and deep-learning tools were employed to analyze ultrastructural changes in synapses, PSD, and dendrites. Our analyses revealed significant decreases in (i) the number of synapses per area or volume (2D or 3D), (ii) SAS, and 3) the volume of PSD in homozygous $App^{NL\text{-}G\text{-}F}$ rats. In addition, the proportion of synapses with mushroom spines was reduced due to an increase in thin spines and a decrease in mushroom spines in these animals. Moreover, there were more inhibitory synapses formed on dendritic shafts in the $App^{NL\text{-}G\text{-}F}$ PFC. Taken together, these results represent an initial attempt to quantitatively depict synaptic deficits at the ultrastructural level in an animal model that closely resembles human AD. Although this study involves only a single brain area with relatively fewer cases, it provides a method of ATUM–SEM combined with AI-assisted 3D reconstruction of the 3D ultrastructure of synapses and dendrites. This approach is particularly beneficial for quantitative measurement of synapses. The result of this study is expected to offer helpful information for the research on AD. Future studies should be directed toward the analysis of synapses from more brain regions, with more cases, at the onset as well as during the progression of the disease.

*[Supplementary material is available at Journal of Molecular Cell Biology online. We thank Lixin Wei, Hongtu Ma, Xiaohui Dong, and Limei Lin (Institute of Automation, CAS) for assistance in EM. We also thank the Core Facilities of Life Science, Peking University, for assistance with Amira software work. We extend special thanks to*

*Zhenchen Li for the critical reading and editing of the manuscript. This work was supported by the Strategic Priority Research Program of the Chinese Academy of Sciences (XDB32030200 to H.H.), the Bureau of International Cooperation, Chinese Academy of Sciences (153D31KYSB20170059 to H.H.), Program of Beijing Municipal Science & Technology Commission (Z201100008420004 to H.H.), CAS Key Technology Talent Program (292019000126 to X.C.), National Key Research and Development Program of China (2017YFE0126500 to B.L.), the National Natural Science Foundation of China (81861138013, 81501105, and 31730034 to B.L.), and Beijing Advanced Innovation Center for Human Brain Protection (to B.L.). Y.J., L.L., K.P., B.L., and H.H. designed the research; Y.J., L.L., and K.P. performed the research; K.P. generated the AD rat model; L.L. performed sample preparation of the WT and AD rats; Y.J. performed imaging, 3D reconstruction, and analysis; X.C. and B.C. performed alignment of the serial images; Y.J., J.Y., L.S., and J.L. performed 3D visualization; Y.J. wrote the manuscript; L.L., K.P., B.L., and H.H. also contributed to the discussion and manuscript writing.]*

Yi Jiang [1,2,†], Linlin Li [1,†], Keliang Pang [3,4,†], Jiazheng Liu [1,5], Bohao Chen [1,2], Jingbin Yuan [1,2], Lijun Shen [1], Xi Chen [1], Bai Lu [3,4], and Hua Han [1,5,6,*]

[1]National Laboratory of Pattern Recognition, Institute of Automation, Chinese Academy of Sciences, Beijing 100190, China
[2]School of Artificial Intelligence, University of Chinese Academy of Sciences, Beijing 101408, China
[3]School of Pharmaceutical Sciences, IDG/McGovern Institute for Brain Research, Tsinghua University, Beijing 100084, China
[4]Beijing Advanced Innovation Center for Structural Biology, School of Life Sciences, Tsinghua University, Beijing 100084, China
[5]School of Future Technology, University of Chinese Academy of Sciences, Beijing 101408, China
[6]Center for Excellence in Brain Science and Intelligence Technology, Chinese Academy of Sciences, Shanghai 200031, China
[†]These authors contributed equally to this work.
*Correspondence to: Hua Han, E-mail: hua.han@ia.ac.cn

**Edited by Jiarui Wu**

## References

Baena, V., Schalek, R.L., Lichtman, J.W., et al. (2019). Serial-section electron microscopy using automated tape-collecting ultramicrotome (ATUM). Methods Cell Biol. *152*, 41–67.

Goedert, M., and Spillantini, M. G. (2006). A century of Alzheimer's disease. Science *314*, 777–781.

Karimi, A., Odenthal, J., Drawitsch, F., et al. (2020). Cell-type specific innervation of cortical pyramidal cells at their apical dendrites. eLife *9*, e46876.

Koffie, R.M., Meyer-Luehmann, M., Hashimoto, T., et al. (2009). Oligomeric amyloid β associates with postsynaptic densities and correlates with excitatory synapse loss near senile plaques. Proc. Natl Acad. Sci. USA *106*, 4012–4017.

Leuner, B., and Shors, T.J. (2013). Stress, anxiety, and dendritic spines: what are the connections? Neuroscience *251*, 108–119.

Motta, A., Berning, M., Boergens, K.M., et al. (2019). Dense connectomic reconstruction in layer 4 of the somatosensory cortex. Science *366*, eaay3134.

Pang, K., Jiang, R., Zhang, W., et al. (2022). An App knock-in rat model for Alzheimer's disease exhibiting Aβ and tau pathologies, neuronal death and cognitive impairments. Cell Res. *32*, 157–175.

Salat, D.H., Kaye, J.A., and Janowsky, J.S. (2001). Selective preservation and degeneration within the prefrontal cortex in aging and Alzheimer's disease. Arch. Neurol. *58*, 1403–1408.

Schikorski, T., and Stevens, C.F. (1997). Quantitative ultrastructural analysis of hippocampal excitatory synapses. J. Neurosci. *17*, 5858–5867.

Serrano-Pozo, A., Frosch, M.P., Masliah, E., et al. (2011). Neuropathological alterations in Alzheimer disease. Cold Spring Harb. Perspect. Med. *1*, a006189.